Journal of Hazardous Materials 192 (2011) 559–567

Contents lists available at ScienceDirect

Journal of Hazardous Materials

journal homepage: www.elsevier.com/locate/jhazmat

Synthesis of sulfated Y-doped zirconia particles and effect on properties of polysulfone membranes for treatment of wastewater containing oil

Yuqing Zhang[a,b,*], Xing Shan[a], Zhenhua Jin[a], Yueling Wang[a]

[a] School of Chemical Engineering and Technology, Tianjin University, Tianjin 300072, China
[b] ARC Centre for Functional Nanomaterials, AIBN and School of Engineering, The University of Queensland, Brisbane 4072, Australia

ARTICLE INFO

Article history:
Received 4 September 2010
Received in revised form 17 May 2011
Accepted 17 May 2011
Available online 26 May 2011

Keywords:
Polysulfone membrane
Sulfated Y-doped zirconia
Hydrophilic property
Anti-fouling property
Anti-compaction capability

ABSTRACT

Polysulfone (PSF) membranes are broadly applied in many fields owing to good physicochemical stability, resistance to oxidation and chlorine. But when treated with wastewater containing oil, PSF membranes are easily contaminated due to their hydrophilicity, causing declining flux and lifespan of the membranes thereby limiting their large scale applications. In order to enhance the hydrophilic and anti-fouling capability of PSF membranes for treating wastewater containing oil, sulfated Y-doped zirconia particles (SO_4^{2-}/ZrO_2–Y_2O_3 or SZY particles) were firstly synthesized and then doped into polysulfone to fabricate a novel hybrid membrane (SZY/PSF). The optimum preparation conditions of SZY particles were studied and determined. SZY particles were characterized by X-ray diffraction (XRD), Fourier transform infrared (FTIR), specific surface area and transmission electron microscopy (TEM). Wastewater containing oil (80 mg/L) was used to investigate the separation properties of SZY/PSF membranes. The results show that the oil concentration in the permeation is 0.67 mg/L, which meets the recycle standard of the Chinese oil-field (SY/T 5329-94, oil concentration <10 mg/L). It is concluded that doping SZY particles into polysulfone can reasonably resist membrane fouling and SZY/PSF membranes can be considered feasible in treating wastewater containing oil.

1. Introduction

A great deal of wastewater containing oil is generated from petrochemical industries, which not only pollutes the environment but also wastes crude oil and water resources. Thus, wastewater containing oil needs to be treated effectively. There are many conventional methods used to treat wastewater, such as gravity setting, flocculating and fiber adsorption. However, soluble oil in the wastewater cannot be entirely eliminated by these methods. Membrane technology offers an effective solution to the problem of treating wastewater containing oil mentioned above [1]. This is because it has a lot of advantages such as easy operation, low cost and capability of reducing contaminants. At present, polysulfone (PSF) membranes are regularly used in the treatment of wastewater containing oil owing to their good physicochemical stability and resistance to oxidation and chlorine [2–6]. However, oil droplets in the wastewater cause PSF membrane fouling, which shortens the lifetime and limits the application area of the PSF membrane [3]. Therefore, enhancing the hydrophilic property and anti-fouling capability of PSF membrane is now the focus of many research groups.

Nowadays many methods to enhance the hydrophilicity of polymer membrane have been reported. Among these methods, doping inorganic oxide particles (such as SiO_2, TiO_2, Al_2O_3, ZrO_2) to polymers to produce organic–inorganic composite membranes is attractive, owing to its simple preparation process and advantages of both organic membranes and inorganic particles [6–9]. Though properties of polymer membranes can be enhanced by adding inorganic oxide particles, further enhancement of polymer membranes' properties is limited. That is because there are few hydroxide radicals on the surface of inorganic oxide particles with stoichiometric structure [10]. In contrast, there are various point defects inside and numerous exposed hydroxide radicals on the surface of non-stoichiometric inorganic oxide particles. So these particles show stronger activity in the course of chemical bonding than inorganic oxide particles with stoichiometric structure [11].

In recent years, materials doped with rare earth elements (such as Ce, La or Y) and materials activated by H_2SO_4 have become two research focuses [12–16]. Zhang et al. [17] prepared the Ce-doped silicas ($Ce_xSi_{1-x}O_{2-\delta-700}$) with $x = 0.06$–0.08 which have the smaller pore size, larger specific surface area, many Lewis acid sites and a better hydrophilic property. Besides, it is reported from the work of Boulouz that proper addition of Y_2O_3 can stabilize tetragonal structure of ZrO_2 which has a higher chemical reaction activity

* Corresponding author at: School of Chemical Engineering and Technology, Tianjin University, Tianjin 300072, China. Tel.: +86 022 2789 0470; fax: +86 022 2740 3389.
E-mail address: zhangyuqing@tju.edu.cn (Y. Zhang).

0304-3894/$ – see front matter © 2011 Elsevier B.V. All rights reserved.
doi:10.1016/j.jhazmat.2011.05.058

at room temperature [18]. Moreover, it is well known that the interaction between sulfated oxides and metals leads to the formation of materials with greater acidity and surface areas than that one of non-sulfated oxides [19]. In the work of Jong et al. [20] and Reddy et al. [21], the surface acidity property of ZrO_2 can be obviously improved by H_2SO_4 activation. Zhang et al. [22] added Ce-doped nonstoichiometric nanosilica to PSF membranes to prepare Ce-doped nonstoichiometric nanosilica/PSF composite membranes and investigated the effect of adding inorganic oxide particles on the improvement of properties of PSF membranes. These reports indicate that doping nonstoichiometric inorganic oxide particles (ZrO_2 or SiO_2) modified by sulfuric acid to polymer membranes may produce composite membranes with better properties. Therefore, studying and developing sulfated nonstoichiometric inorganic oxide particles have important significance to enhance the hydrophilic property, antifouling capability, tensile strength and anti-compaction property of PSF membranes.

In this paper, in order to enhance the hydrophilic and antifouling capability of PSF membranes for treating wastewater containing oil, SZY particles were firstly synthesized and then doped into PSF to fabricate SZY/PSF membranes by a sol–gel process. The optimum preparation conditions of SZY particles were studied and determined; SZY particles were characterized by XRD, FTIR, Specific surface area and TEM etc.; the hydrophilic property, antifouling capability, tensile strength and anti-compaction property of SZP/PSF membranes were also investigated.

2. Experimental

2.1. Materials and reagents

Y_2O_3, $ZrOCl_2{\cdot}8H_2O$, SiO_2 and nonionic surfactant – fatty alcohol polyoxyethylene ether (SA-20) were obtained from Tianjin Jiangtian Chemical Technology Co. Ltd. (China). N-Butyl alcohol and $NH_3{\cdot}H_2O$ were supplied by Tianjin Jinyu Fine Chemical Factory (China). PSF was purchased from Dalian Polysulfone Co. Ltd. (China); its MW and polydispersity were 84,400 Da and 1.37, respectively.

2.2. Preparation of SZY particles and SZY/PSF membrane

2.2.1. Preparation of SZY particles

Y_2O_3, $ZrOCl_2{\cdot}8H_2O$ and surfactant SA-20 with different molar ratios were dissolved in a hydrochloride solution of 1 mol/L under stirring while heating at 40–50 °C. Aqueous ammonia of 2 mol/L was then added into the mixed solution until the pH value was adjusted to about 10.0. After aging for 12 h at 25 °C, the ZrO_2–Y_2O_3 gel particles were washed with deionized water to remove chloride ions. After chloride ions removal, ZrO_2–Y_2O_3 gel particles were washed with n-butyl alcohol for several times and vacuum dried at 110 °C to form ZrO_2–Y_2O_3 powder particles. Then the ZrO_2–Y_2O_3 powder particles were dipped in H_2SO_4 solutions of different concentration while stirring for 30 min, filtered by the Buchner funnel, dried at 110 °C and finally sintered at different temperatures for 2 h. Finally, a series of SZY particles with yttrium of different molar ratio were obtained.

2.2.2. Preparation of SZY/PSF membrane

The preparation process of the membranes is similar to the literature [23]. In this paper, SZY particles were used as the filling materials to prepare the SZY/PSF membrane (the mass ratio of SZY/PSF was 15%). The PSF membrane and SiO_2/PSF membrane (the mass ratio of SiO_2/PSF was also 15%) were used as comparison samples.

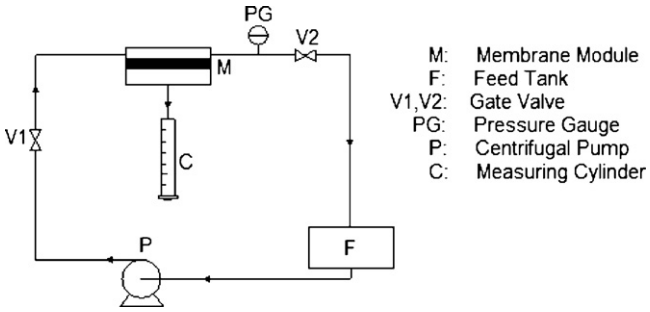

Fig. 1. Schematic diagram of the experimental device.

2.3. Characterization of SZY particles and SZY/PSF membrane

XRD measurement of SZY particles was performed using a D8 Advance X-ray diffraction (Bruker Corporation, Germany) with Co K_α ($\lambda = 0.17890$ nm) radiation, a scanning range (2θ) from 10° to 90°, the sampling pitch 0.02°, the tube voltage 40 kV and the tube electric current 40 mA. Samples were tested after grinding and pressing a tablet.

Specific surface area of SZY particles was determined by a NOVA-2000 specific surface area and porosity analyzer (Quantachrome Instruments, USA).

SZY particles were investigated by the Nicolet NEXUS Fourier transform infrared (FTIR) spectra (Thermo Scientific Corporation, USA), by the KBr method, with Acc Voltage 10 kV. And the TEM images of the samples were recorded on a JEM-100CX II transmission electron microscope (JEOL Corporation, Japan) with the operating voltage of 100 kV.

Membrane surfaces and cross-section were observed under a Nanosem 430 scanning electron microscope (FEI Corporation, USA) with the voltage of 10 kV. An even specimen of fabricated membrane was tested with an Instron 5543 material extensometer (Instron Corporation, USA). The operation conditions were stroke speed 15 mm/min, measuring range 0–4 MPa and test temperature 21 °C.

2.4. Studies of properties of membranes doped with SZY particles

2.4.1. Anti-compaction experiment of membranes

It is known that both membrane contamination and membrane compaction lead to flux changes. Because pure water was used as the feed solution in this experiment, the negative effect of membrane contamination on the flux of membrane was eliminated. Therefore, the anti-compaction property of SZY/PSF membrane, SiO_2/PSF membrane and PSF membrane can be evaluated by the pure water flux of these membranes. Fig. 1 shows a schematic diagram of the experimental set-up used in this paper. Feed solution (pure water) was transported to the membrane groupware by a diaphragm pump. Flow was regulated using a valve V1 while the pressure on the membrane was adjusted by another valve V2. The feed stream split into two streams: the one which contained non-passing components was returned to the feed tank; the other one contained components passing through the membrane and it was measured by a measuring cylinder. The permeation was returned to the feed tank in order to keep a constant feed concentration. The permeation volume of pure water was recorded per 1 h and the operating pressure was 0.20 MPa. Permeation flux of pure water is calculated by the following equation:

$$J = \frac{V}{S \cdot t} \quad (1)$$

where J is the permeation flux (L/(m^2 h)), V the permeation volume (L), S the effective membrane area (m^2) and t the operating time.

After a certain time, flux declination occurred and it can be calculated by the equation:

$$\mathrm{FD} = \frac{J_0 - J_t}{J_0} \times 100\% \quad (2)$$

where FD is the flux declination (%), J_0 is the initial permeation flux (L/(m^2 h)) and J_t is the permeation flux at t time (L/(m^2 h)).

2.4.2. Hydrophilicity experiment of membranes

The permeation flux test of membranes for wastewater containing oil was carried out under the operating pressure of 0.20 MPa for 11 h (oil concentration of the wastewater is 80 mg/L). To take into consideration the negative effect of membrane compaction on the flux of the membrane, SZY/PSF membrane, SiO_2/PSF membrane and PSF membrane which had been operated for 30 h in the anti-compaction experiment were used in this hydrophilicity experiment. Thereby, the permeation flux of membranes can be used to represent the hydrophilicity of membranes. The experimental set-up was the same as used in the anti-compaction experiment (Fig. 1) and the procedure was similar with that in the anti-compaction experiment except wastewater containing oil was used as the feed solution in the permeation flux experiment.

The oil concentration in the permeation was determined by UV spectrophotometer (PE Co. Ltd., USA) at 225 nm [24,25] and the retention rate R is calculated by the following equation:

$$R = \frac{(C_1 - C_2)}{C_1} \times 100\% \quad (3)$$

where R is the retention rate (%), C_1 the oil concentration in the feed solution (80 mg/L) and C_2 the oil concentration in the permeation (mg/L).

Moreover, membranes without compaction treatment were tested by the 1501 type contact anglometer (Micromeritics Corporation, USA) in order to show the hydrophilicity of these membranes.

2.4.3. Permeation flux recovery experiment of membranes

After working for a period, the permeation flux of membrane tends to decline and can recover to some degree by the flushing process. The filling effect of SZY particles on the integrative properties of PSF membrane including the hydrophilic property, antifouling capability and anti-compaction property was investigated via the permeation flux recovery of membranes after backflushing and chemical cleaning.

The operating conditions for the backflushing experiment were: backflushed once after each 11 h for one 20 min period; the operating condition for chemical cleaning experiment was: chemical cleaning once every month for one 30 min period. The chemical cleaning process was as follows:

(1) Clean membranes with 3% NaOH solution, and then rinse with pure water.
(2) Clean membranes with 3% HCl solution, and then rinse with pure water to obtain a neutral state.

The permeation flux recovery of membranes experiment was carried out at the condition of oil concentration of wastewater 80 mg/L, temperature 25 °C and operating pressure 0.20 MPa.

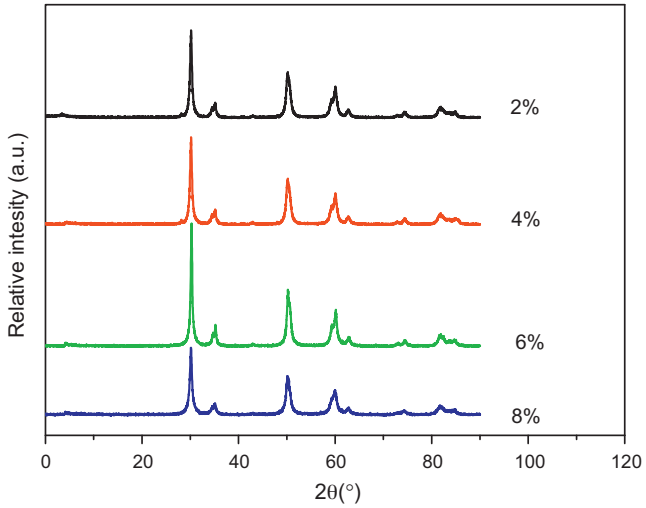

Fig. 2. X-ray diffraction patterns of SZY particles doped with molar ratios of yttrium/zirconium 2%, 4%, 6% and 8%.

3. Results and discussion

3.1. Determination of optimum preparation conditions for SZY particles

3.1.1. Effect of the yttrium element concentration

As shown in Fig. 2, X-ray diffraction peaks of SZY particles at $2\theta = 30.15°$, $35.18°$ and $50.56°$ can be observed, attributed to crystal face (1 1 1), (2 0 0) and (2 2 0) of the tetragonal ZrO_2 phase respectively [26]. It is also observed from Fig. 2 that when the molar ratio of yttrium/zirconium is 6%, the diffraction peaks for tetragonal ZrO_2 system are strongest, which suggests that the content of tetragonal ZrO_2 phase in SZY particles reaches the maximum [27]. However, the diffraction peaks weaken when the molar ratio of yttrium/zirconium exceeds 6% and there is no diffraction peak of Y_2O_3 in X-ray diffraction patterns of particles, which shows that the Y^{3+} cations have been doped into the frame structure of ZrO_2. It can be determined from the results that the appropriate molar ratio of yttrium/zirconium is 6% and this is the appropriate concentration of yttrium element that can inhibit the crystal transition of ZrO_2 system from tetragonal phase to monoclinic phase.

3.1.2. Effect of the surfactant concentration and H_2SO_4 solution concentration

In this paper, nonionic surfactant SA-20 with hydrophobic aliphatic alcohol and hydrophilic epoxyethane was used to prepare SZP particles. The size and specific surface area of SZY particles controlled by the concentration of surfactant SA-20 and H_2SO_4 solution were studied. Results are shown in the Table 1 and Fig. 3, respectively. The average particle size of SZY particles is calculated by the Scherrer formula:

$$D = \frac{K\lambda}{\beta \cos\theta} \quad (4)$$

Table 1
Effects of the surfactant SA-20 concentration on properties of SZY particles.

No.	Surfactant concentration (wt%)	Specific surface area (m^{2}g^{-1})	Average particle size (nm)
1	1	165.3	53
2	3	220.8	36
3	5	210.6	45
4	7	172.4	50

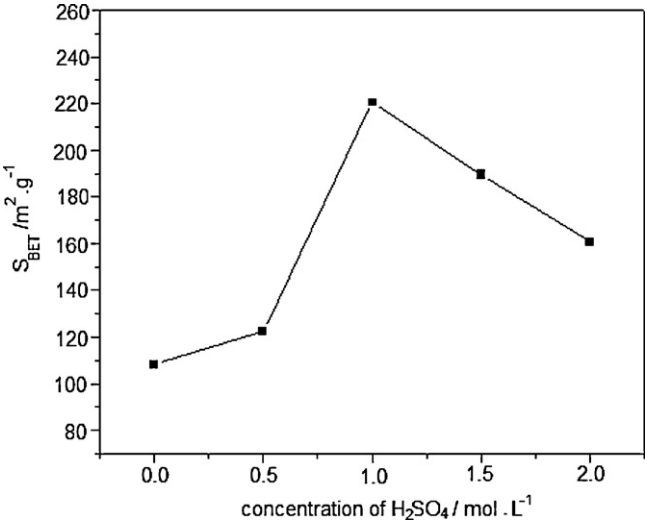

Fig. 3. Effect of H_2SO_4 solution concentration on specific surface area of SZY particles.

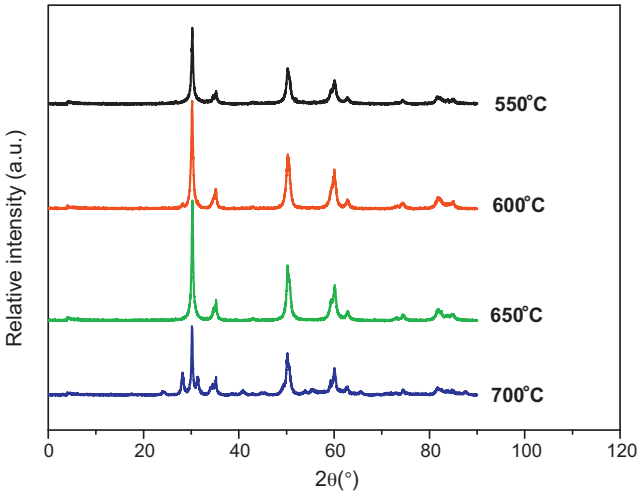

Fig. 4. X-ray diffraction patterns of SZY particles sintered at different temperatures (the molar ratio of yttrium/zirconium is 6%).

where D is the average diameter of particles; λ is the X-ray wavelength; K is a constant 0.89; β is the half peak width of X-ray diffraction peak at $2\theta = 30.15^\circ$.

As it is shown in Table 1, when the surfactant SA-20 concentration is 3 wt%, the average particle size of SZY particles reaches the minimum value 36 nm and the specific surface area of SZY particles reaches the maximum value 220.8 $m^2\,g^{-1}$. In order to synthesize SZY particles with better properties, the appropriate concentration of surfactant SA-20 is 3 wt%.

Moreover, it can be observed from Fig. 3 that when H_2SO_4 solution concentration is less than 1.0 mol/L, the specific surface area of SZY particles increases rapidly with increasing of H_2SO_4 solution concentration. This is because aggregation between SZY particles can be effectively inhibited when the concentration of H_2SO_4 solution is less than 1.0 mol/L. In contrast, when H_2SO_4 solution concentration is more than 1.0 mol/L, the superfluous H_2SO_4 can react with ZrO_2 to form $Zr(SO_4)_2$ [28]. After sintering, $Zr(SO_4)_2$ can decompose and generate ZrO_2 which causes SZY particles to aggregate. Thereby, the specific surface area of SZY particles decreases rapidly when the H_2SO_4 solution concentration exceeds 1.0 mol/L. So the appropriate concentration of H_2SO_4 solution is 1.0 mol/L, because under this condition the maximum surface area of SZY particles can be obtained.

3.1.3. Effect of sintering temperature

Fig. 4 represents the X-ray diffraction patterns of SZY particles that were sintered at different temperatures for 2 h. The molar ratio of yttrium/zirconium is 6%. It can be observed from Fig. 4 that when sintering temperature reaches 700 °C, characteristic diffraction peaks of monoclinic SZY particles system ($2\theta = 28.16^\circ$ and $2\theta = 31.44^\circ$) appear and the characteristic peaks of tetragonal SZY particles system ($2\theta = 30.15^\circ$) weaken significantly. This result suggests that some SZY particles have changed from tetragonal phase to monoclinic phase. In addition, the characteristic diffraction peaks of the tetragonal SZY particles system (at $2\theta = 30.15^\circ$) are strongest at 650 °C, which suggests that the appropriate sintering temperature of SZY particles should be 650 °C. Furthermore, based on the report that pure ZrO_2 crystal is in a tetragonal phase at 1100–2300 °C [26], the analyses above show that adding yttrium and introducing SO_4^{2-} group could prevent the transition of SZY particles from tetragonal phase to monoclinic phase at low temperatures.

The average particle size, the specific surface area of SZY particles and sulfur content on the surface of SZY particles sintered at different temperature for 2 h were measured and results are shown in Table 2. With increasing sintering temperature, the average size of SZY particles increases gradually whereas their specific surface area and sulfur content decrease gradually. When the sintering temperature is higher, SZY particles can melt and aggregate to form larger particles, which finally results in the increase of particle size and the decrease of specific surface area. According to the analyses above, the optimum sintering temperature of SZY particles is 650 °C.

It can be determined from analyses above that optimum preparation conditions for SZY particles are: the molar ratio for yttrium/zirconium 6%, the surfactant SA-20 concentration 3 wt%, the H_2SO_4 concentration 1 mol/L and the sintering temperature 650 °C for 2 h.

3.2. FTIR analysis of sample particles

SZY particles (these particles were prepared under the optimum conditions listed previously: molar ratio yttrium/zirconium 6%, surfactant SA-20 concentration 3 wt% and H_2SO_4 concentration 1 mol/L) were characterized by FTIR.

The FTIR spectra of particles are shown in Fig. 5. The peaks at 3400 cm^{-1} and 1627 cm^{-1} are attributed to the stretching vibration and distorting vibration of OH group, respectively. Compared with FTIR spectra for ZrO_2 particles, the characteristic vibration peaks of OH group for SZY particles are stronger. A stretching vibration peak of Zr–O–Zr bond of ZrO_2 particles is at 500 cm^{-1} (a); in contrast, stretching vibration peaks of Zr–O–Zr bond of SZY particles are at 460 cm^{-1} (b) and 469 cm^{-1} (c), respectively, which move toward the lower wave number region. These results indicate that Zr–O–Y bond is formed and the Y^{3+} cations are doped into the ZrO_2 frame structure [29]. The conclusion is in accord with the conclu-

Table 2
Effect of sintering temperature on properties of SZY particles.

T (°C)	Sintering time (h)	Average particle size (nm)	Specific surface area ($m^2\,g^{-1}$)	SO_3 (wt%)
550	2	14	264.1	7.9
600	2	23	240.3	5.1
650	2	36	220.8	3.6
700	2	69	113.5	2.3
800	2	86	78.03	1.1

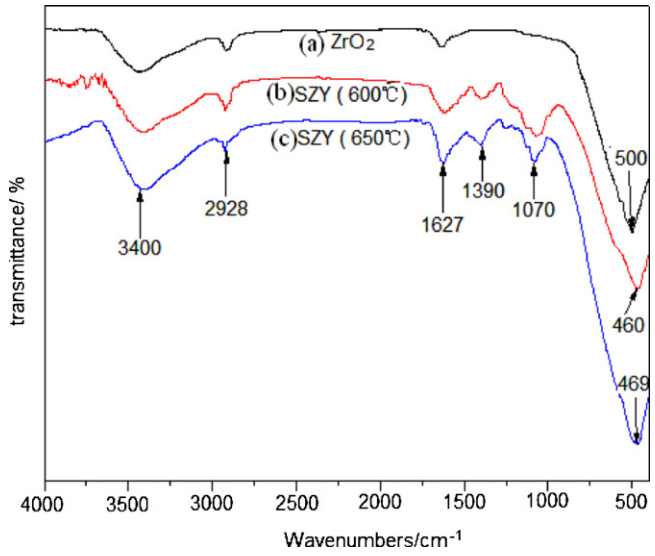

Fig. 5. FTIR spectra of ZrO_2 particles, SZY particles sintered at 600 °C and 650 °C respectively.

sion of X-ray diffraction patterns of SZY particles in Fig. 2. The weak absorption band at 2928 cm^{-1} is the characteristic peak of ZrO_2. It is also observed in the FTIR spectrum (b) and (c) [30]. The peak of S=O covalent band at 1390 cm^{-1} is a characteristic peak of H_2SO_4 and the bands at 1070 cm^{-1} are assigned to a chemical bond formed by chelate reactions between sulfate and metal ions on the surface of the ZrO_2. These results suggest that Y^{3+} cations have entered into the ZrO_2 frame structure and partly replaced Zr^{4+} cations inside the ZrO_2. Furthermore, it is reported that the characteristic peak strength of the Lewis acid site (around 1450 cm^{-1}) and the Brønsted acid site (around 1530–1550 cm^{-1}) are reduced at 423 K with the comparison of those at 298 K [31]. When the sintering temperature exceeds 600 °C, the two characteristic peaks will gradually disappear. Therefore, they are not observed in spectrum (b) and (c).

3.3. TEM analysis of sample particles and SEM of SZY/PSF membrane

When preparing SZY particles for TEM analysis, ZrO_2–Y_2O_3 gel particles were first washed by deionized water, then were dipped in H_2SO_4 solution, dried and sintered, respectively. Finally, SZY particles (a) were obtained. Similarly, SZY particles (b) were obtained by following procedure: ZrO_2–Y_2O_3 gel particles were firstly washed by deionized water and n-butyl alcohol, dipped in H_2SO_4 solution, dried and sintered, respectively. SZY particles (a) and (b) were synthesized under the optimum preparation conditions: the molar ratio for yttrium/zirconium 6%, the surfactant SA-20 concentration 3 wt%, the H_2SO_4 concentration 1 mol/L and the sintering temperature 650 °C for 2 h.

Table 3
Tensile strength of pure PSF, 15 wt% SiO_2/PSF and 15 wt% SZY/PSF membranes.

Type of membrane	Tensile strength (MPa)
Pure PSF membrane	1.925
15 wt% SiO_2/PSF membrane	2.101
15 wt% SZY/PSF membrane	3.315

Fig. 6(a) shows the TEM images of SZY particles (a) washed by deionized water; Fig. 6(b) shows the TEM images of SZY particles (b) washed with deionized water and n-butyl alcohol. It can be seen from Fig. 6 that SZY particles are basically spherical shape with the particle diameter between 30 nm and 50 nm. Furthermore, it is apparent that sample (a)'s aggregation is stronger than that of sample (b) and sample (a) particles disperse unevenly. It is because that after washing with n-butyl alcohol, ZrO_2–Y_2O_3 gel particles adsorb the layers of n-butyl alcohol to inhibit the aggregation between SZY particles. In addition, when ZrO_2–Y_2O_3 gel particles are sintered, n-butyl alcohol molecules (boiling point at 117.7 °C) decomposed into gas molecules to form space steric hindrance, which also effectively inhibits the aggregation between SZY particles.

Fig. 7 shows the SEM images of the cross section and surface of the 15 wt% SZY/PSF membrane. It is observed in Fig. 7(a)–(c) that dispersibility of SZY particles in the PSF membrane is relatively uniform. In addition, it indicates from Fig. 7(a) that SZY particles are doped into the PSF membrane structure and have good compatibility with the PSF membrane, which can improve the tensile strength and anti-compaction capability of the hybrid membrane. As indicated from Fig. 7(b) SZY particles disperse on the top surface of the hybrid membrane and addition of SZY particles causes the surface of the SZY/PSF membrane to appear a little rough.

3.4. Anti-compaction test of membrane

It can be observed from Fig. 8 that the pure water flux of membranes decreases rapidly at the initial stage, then changes slowly after operating for about 2 h. The pure water flux for SZY/PSF hybrid membrane at the steady stage (125.6 L/(m^2 h)) is the highest among the three kinds of membranes, which suggests that SZY/PSF hybrid membrane gains better anti-compaction properties than SiO_2/PSF and PSF membranes. The tensile strength of the three membranes is shown in Table 3. The tensile strength of membranes is improved from 1.925 MPa to 3.315 MPa and tensile strength of the SZY/PSF membrane is higher than SiO_2/PSF membranes (2.101 MPa). It is because the dispersion property and polysulfone compatibility of SZY particles in the hybrid membrane is better than SiO_2 parti-

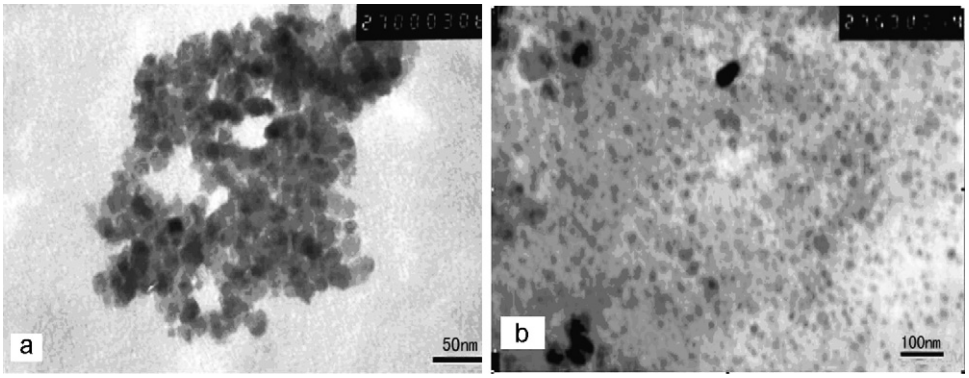

Fig. 6. TEM images of SZY particles with molar ratio of yttrium/zirconium 6% and sintered at 650 °C (magnification: (a) ×140,000; (b) ×70,000).

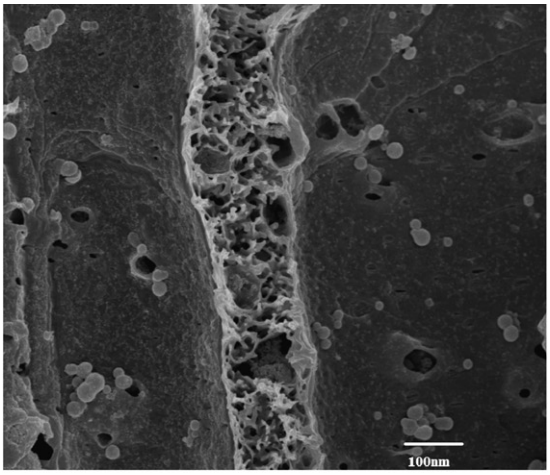

(a) Cross section

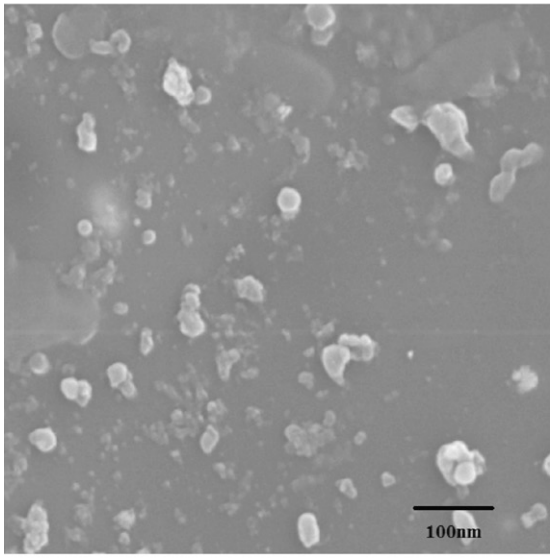

(b) Top surface

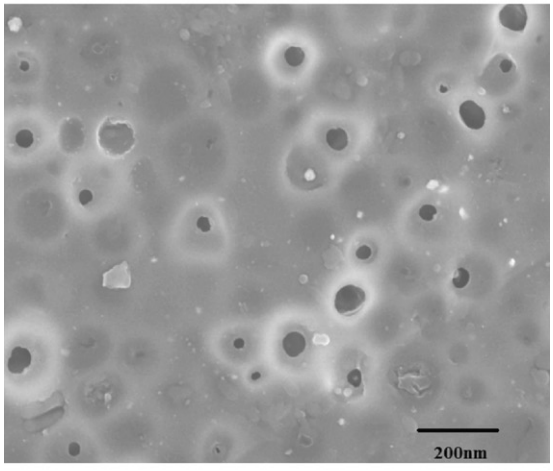

(c) Bottom surface

Fig. 7. SEM of the cross section and surface of the 15 wt% SZY/PSF membrane: (a) cross section ×60,000, (b) top surface ×60,000, (c) bottom surface ×30,000.

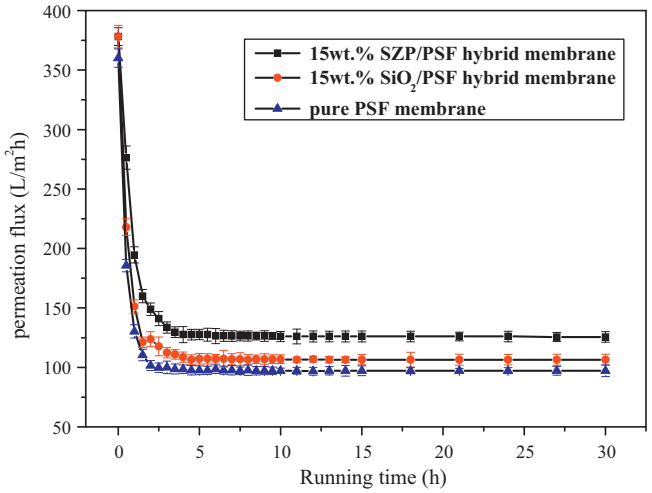

Fig. 8. Permeation flux of different membranes for pure water.

cles. Results show that doping SZY particles into PSF membranes effectively improves mechanical performance and anti-compaction properties of the SZY/PSF hybrid membrane.

3.5. Hydrophilicity test of membrane

Fig. 9 shows the relationship of permeation flux of compressed membranes and operation time when treating wastewater containing oil. Permeation flux of SZY/PSF membrane for wastewater containing oil reaches steady state (110 L/(m^2 h)) after operating for 8 h, which is higher than that of SiO_2/PSF and PSF membranes (90 L/(m^2 h) and 60 L/(m^2 h), respectively). FD of SZY/PSF, SiO_2/PSF and PSF membranes at 11 h is 53.25%, 54.58% and 60% respectively. It is reported that as time extends, the membrane resistance caused by membrane surface fouling is the main reason for the flux decline [2]. It can be observed that FD of SZY/PSF membrane is minimum, which exactly shows that doping SZY particles into PSF membrane can improve hydrophilic properties of the SZY/PSF membrane to decrease membrane fouling. It is because SZY particles with more OH groups and Lewis acid sites are dispersed inside SZY/PSF hybrid membrane, which makes SZY/PSF hybrid membrane have better hydrophilic properties. Table 4 shows the results of water samples treated by different membranes for 11 h. The oil concentration in permeation treated by the SZY/PSF membrane is 0.67 mg/mL, which

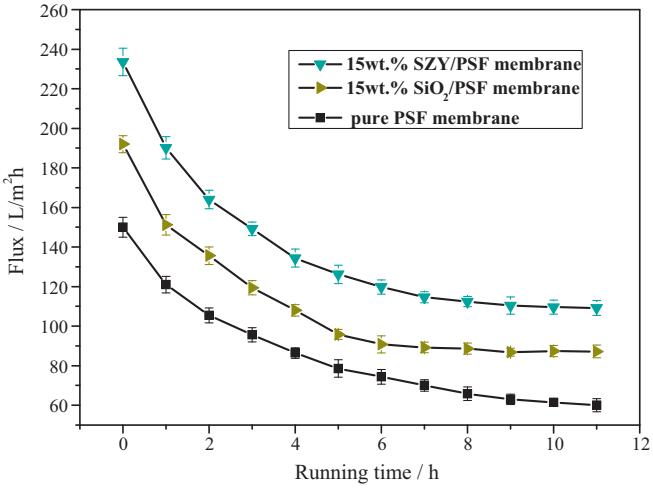

Fig. 9. Permeation flux of different compressed membranes for wastewater containing oil.

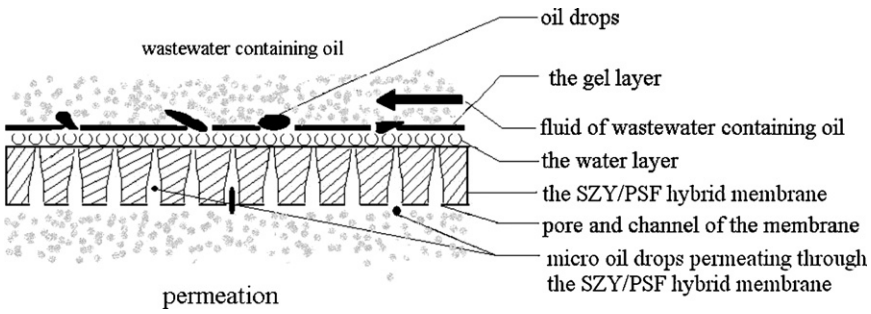

Fig. 10. The anti-fouling mechanism of the SZY/PSF hybrid membrane.

meets the recycle standard of Chinese oil-filed (SY/T 5329-94, oil concentration <10 mg/L). The results indicate that SZY/PSF membranes have a potential application in treatment of wastewater containing oil.

It can be also observed from Fig. 10 that when wastewater containing oil flow through the surface of the hybrid membrane, a water layer is formed between water molecules and SZY particles by hydrogen bond, which can effectively inhibit oil drops to pass through the hybrid membrane. After operating for a period, the gel layer formed on the surface of the water layer was accumulated to a certain thickness and easily washed off by wastewater. With extended operation time, this procedure promotes the SZY/PSF hybrid membrane to obtain hydrophilicity and antifouling properties. The analyses above suggest that the SZY/PSF hybrid membrane has a potential application in treating wastewater containing oil due to its strong hydrophilic property and anti-fouling capability.

In order to further validate the effect of SZY particles on the hydrophilic property of membranes, the contact angles of membranes were tested and results were presented in Fig. 11. As it is shown in Fig. 11, the contact angle of membranes reduces from 78.1° to 45.2° and the contact angle of SZY/PSF membrane is less than that of the SiO_2/PSF membrane. It indicates that doping particles into PSF membrane can improve the hydrophilic property of membrane and the hydrophilic property of SZY/PSF membrane is best among the three kinds of membranes. It is because that there are more OH groups on the surface of SZY particles than that on the surface of SiO_2 particles. Furthermore, after the Y^{3+} cations replace some Zr^{4+} cations in the ZrO_2 crystal lattice, more oxygen vacancies and defects are generated. And more Lewis acid sites are generated after combining SO_4^{2-} group with ZrO_2, which enhances hydrophilic capability of the SZY/PSF membrane.

3.6. Effects of backflushing and chemical cleaning on permeation flux of membranes

It is observed from Figs. 8 and 9 that with extending operation time, the flux of membranes declines. It is mainly due to the membrane fouling caused by both the cake layer (the effect that backflushing can decrease) and adsorption or pore plugging (the effect that backflushing cannot decrease) [32]. Results of permeation flux recovery after backflushing are shown in Fig. 12. The final permeation flux of SZY/PSF membrane for wastewater con-

Table 4
Results of water samples after treatment.

Membrane	Oil concentration in the permeation (mg/L)	Oil retention rate (%)
Oil concentration in the feed solution	80.00	–
PSF membrane	5.00	93.75
15%SiO_2/PSF membrane	2.68	96.65
15%SZY/PSF membrane	0.67	99.16

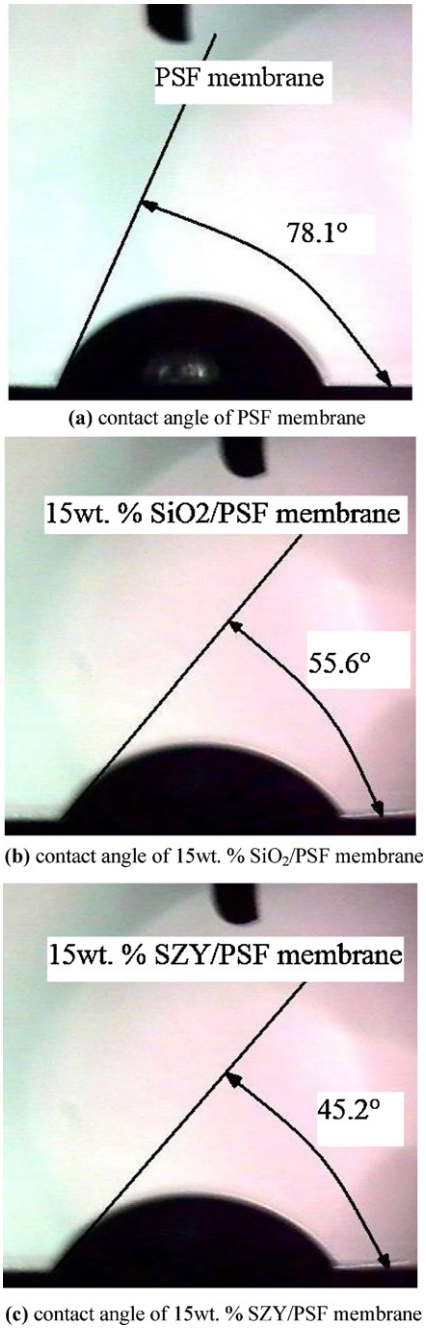

(a) contact angle of PSF membrane

(b) contact angle of 15wt. % SiO_2/PSF membrane

(c) contact angle of 15wt. % SZY/PSF membrane

Fig. 11. (a) Contact angle of PSF membrane. (b) Contact angle of 15 wt% SiO_2/PSF membrane. (c) Contact angle of 15 wt% SZY/PSF membrane.

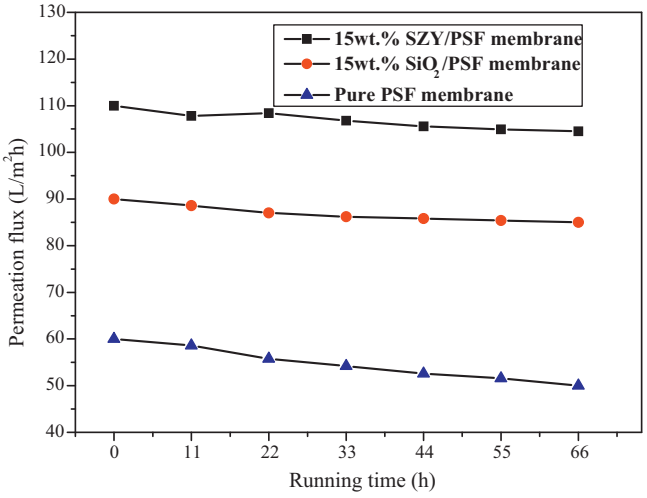

Fig. 12. Effect of backflushing on permeation flux recovery of membranes for wastewater containing oil.

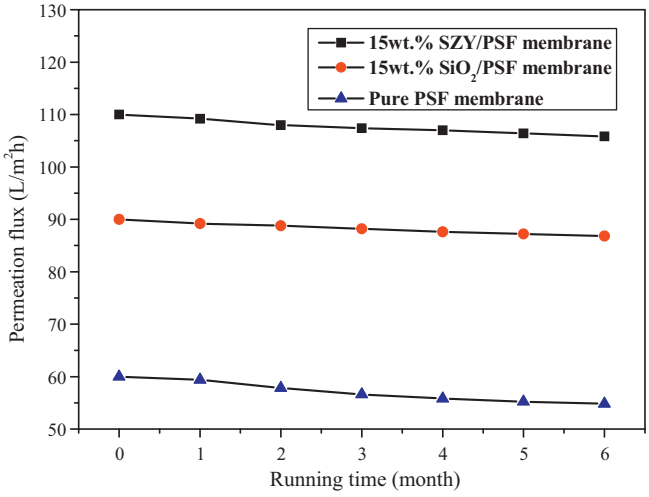

Fig. 13. Effect of chemical cleaning on permeation flux recovery of membranes for wastewater containing oil.

taining oil is 104.5 L/(m^2 h) and FD is 5% which is less than that of both SiO_2/PSF and PSF membranes. These results indicate that backflushing can effectively restore the flux of SZY/PSF membrane to its original level. This is because stronger hydrophilicity of SZY particles can decrease the PSF membrane fouling caused by the cake layer, which is already explained in 3.5.

Results of permeation flux recovery after chemical cleaning are shown in Fig. 13. Comparing with both PSF and SiO_2/PSF membranes, the SZY/PSF membrane has a better capability of flux recovery. It indicates that chemical cleaning has a positive effect on resuming the permeation flux of membranes and hence producing SZY/PSF membrane with a long service life which can be recycled. Therefore, SZY/PSF membranes have potential practical applications in treating wastewater containing oil.

4. Conclusions

The optimum preparation conditions of SZY particles are: the molar ratio for yttrium/zirconium 6%, the surfactant SA-20 concentration 3 wt%, the H_2SO_4 concentration 1 mol/L and the sintering temperature 650 °C for 2 h. The appropriate addition of yttrium element and introducing SO_4^{2-} group can prevent the transition of SZY particles from the tetragonal system to the monoclinic system. SZY particles improve the anti-compaction property of SZY/PSF hybrid membranes. After backflushing and chemical cleaning, the permeation flux recovery of SZY/PSF membrane was better than SiO_2/PSF and PSF membranes. Therefore, SZY/PSF hybrid membranes with strong hydrophilic properties and antifouling capability have potential practical applications in treating wastewater containing oil.

Acknowledgements

This project is supported by the National Natural Science Foundation of China (No. 21076143), the Scientific Research Foundation for the Returned Overseas Chinese Scholars, State Education Ministry (No. 2009-1341), the Basic Research of Tianjin Municipal Science and Technology Commission (No. 07JCYBJC00700), the Key Laboratory of Inorganic coating materials, Chinese Academy of Sciences (No. KLICM-2010-06) and the Program of Introducing Talents of Discipline to Universities (No. B06006).

References

[1] F. Ahmadun, A. Pendashteh, L.C. Abdullah, D.R.A. Biak, S.S. Madaeni, Z.Z. Abidin, Review of technologies for oil and gas produced water treatment, J. Hazard. Mater. 170 (2009) 530–551.
[2] B. Chakrabarty, A.K. Ghoshal, M.K. Purkait, Ultrafiltration of stable oil-in-water emulsion by polysulfone membrane, J. Membr. Sci. 325 (2008) 427–437.
[3] H. Ju, B.D. McCloskey, A.C. Sagle, Y.H. Wu, Crosslinked poly(ethylene oxide) fouling resistant coating materials for oil/water separation, J. Membr. Sci. 307 (2008) 260–267.
[4] Y.N. Yang, H.X. Zhang, P. Wang, The influence of nano-sized TiO2 fillers on the morphologies and properties of PSF UF membrane, J. Membr. Sci. 288 (2007) 231–238.
[5] F.R. Ahmadun, A. Pendashteha, L.C. Abdullah, Review of technologies for oil and gas produced water treatment, J. Hazard. Mater. 170 (2009) 530–551.
[6] S.P. Nunes, K.V. Peinemann, K. Ohlrogge, et al., Membranes of poly (ether imide) and nanodispersed silica, J. Membr. Sci. 157 (1999) 219–226.
[7] Y.G. Jin, S.Z. Qiao, J.C.D. Costa da, B.J. Wood, B.P. Ladewig, G.Q. Lu, Hydrolytically stable phosphorylated hybrid silicas for proton conduction, Adv. Funct. Mater. 17 (2007) 3304–3311.
[8] Y.F. Zhai, H.M. Zhang, J.W. Hu, B.L. Yi, Preparation and characterization of sulfated zirconia (SO_4^{2-}/ZrO_2)/Nafion composite membranes for PEMFC operation at high temperature/low humidity, J. Membr. Sci. 280 (2006) 148–155.
[9] R.A. Damodar, S.J. You, H.H. Chou, Study the self cleaning, antibacterial and photocatalytic properties of TiO_2 entrapped PVDF membranes, J. Hazard. Mater. 172 (2009) 1321–1328.
[10] V.P. Zlomanov, A.J. Zavrazhnov, A.V. Davydov, Nonstoichiometry and P–T–x diagrams of binary systems, Intermetallics 11 (2003) 1287–1291.
[11] G.G. Libowitz, J.B. Lightstone, Characterization of point defects in nonstoichiometric compounds from thermodynamic considerations, J. Phys. Chem. Solids 28 (1967) 1145–1154.
[12] H. Matsuhashi, H. Shibata, H. Nakamura, K. Arata, Skeletal, isomerization mechanism of alkanes over solid superacid of sulfated zirconia, Appl. Catal. A: Gen. 187 (1999) 99–106.
[13] J.A. Moreno, G. Poncelet, Isomerization of *n*-butane over sulfated Al and Ga-promoted zirconium oxide catalysts. Influence of promoter and preparation method, J. Catal. 203 (2001) 453–465.
[14] H.Z. Ma, F.T. Chen, B. Wang, Q.F. Zhuo, Modified SO_4^{2-}/Fe_2O_3 solid superacid catalysts for electrochemical reaction of toluene with methanol, J. Hazard. Mater. 145 (2007) 453–458.
[15] B. Cina, I. Eldror, Bonding of stabilised zirconia (Y-TZP) by means of nano Y-TZP particles, Mater. Sci. Eng. A 301 (2001) 187–195.
[16] M. Scheithauer, R.K. Grasselli, H. Kno'zinger, Genesis and structure of WO_x/ZrO_2 solid acid catalysts, Langmuir 14 (1998) 3019–3029.
[17] Y.Q. Zhang, T.D. Du, Study on Ce-doped nonstoichiometric nanosilica for promoting properties of polysulfone membranes, Chem. Eng. Technol. 33 (2010) 676–681.
[18] M. Boulouz, A. Boulouz, A. Giani, et al., Influence of substrate temperature and target composition on the properties of yttria-stabilized zirconia thin films grown by r.f. reactive magnetron sputtering, Thin Solid Films 323 (1998) 85–92.
[19] R. Silva Rodrigo, J.M. Hernández Enríquez, A. Castillo Mares, J.A. Melo Banda, R. García Alamilla, M. Picquart, T. López Goerne, Effect of CeO_2 on the textural and acid properties of ZrO_2–SO_4^{2-}, Catal. Today 107–108 (2005) 838–843.
[20] R.S. Jong, H.L. Si, S.L. Jun, New solid superacid catalyst prepared by doping ZrO_2 with Ce and modifying with sulfate and its catalytic activity for acid catalysis, Catal. Today 116 (2006) 143–150.
[21] B.M. Reddy, P.M. Sreekanth, P. Lakshmanan, et al., Synthesis,characterization and activity study of $SO_4^{2-}/Ce_xZr_{1-x}O_2$ solid superacid catalyst, J. Mol. Catal. 244 (2006) 1–7.

[22] Y.Q. Zhang, L.B. Shan, Z.Y. Tu, Y.H. Zhang, Preparation and characterization of novel Ce-doped nonstoichiometric nanosilica/polysulfone composite membranes, Sep. Purif. Technol. 63 (2008) 207–212.
[23] Y.Q. Zhang, X.Q. Gao, Y.L. Wang, Study on the build of channels in accurate separation membrane and its selective mechanism, J. Membr. Sci. 339 (2009) 100–108.
[24] X. Zhao, Y.M. Wang, Z.F. Ye, Oil field wastewater treatment in Biological Aerated Filter by immobilized microorganisms, Process Biochem. 41 (2006) 1475–1483.
[25] X.M. Chen, G.H. Chen, P.L. Yue, Separation of pollutants from restaurant wastewater by electrocoagulation, Sep. Purif. Technol. 19 (2000) 65–76.
[26] Y.Y. Zhan, G.H. Cai, Y.H. Xiao, Diffusion reflectance spectroscopy of ZrO_2 phase structure, Spectrosc. Spectral. Anal. 24 (2004) 914–917.
[27] P. Li, I.W. Chen, E.P.H. James, X-ray-absorption studies of zirconia polymorphs: I. Characteristic local structures, effect of Y_2O_3 dopant on ZrO_2 structure, Phys. Rev. B 48 (1993) 10063–10081.
[28] C.X. Miao, Z. Gao, Preparation and properties of ultrafine SO_4^{2-}/ZrO_2 superacid catalysts, Mater. Chem. Phys. 50 (1997) 15–19.
[29] G. Larsen, E. Lotero, L.M. Petkovic, D.S. Shobe, Alcohol dehydration reactions over tungstated zirconia catalysts, J. Catal. 169 (1997) 67–75.
[30] J.C. Cao, X.L. Zhou, Z.C. Guo, Y.Y. Fan, D.G. Deng, Preparation and properties of ZrO_2 coating on stainless steel, Mater. Mech. Eng. 28 (2004) 29–31.
[31] S. Damyanova, P. Grange, B. Delmon, Surface characterization of zirconia-coated alumina and silica carriers, J. Catal. 168 (1997) 421–430.
[32] J. Cakl, I. Bauer, P. DoleČek, Effects of backflushing conditions on permeate flux in membrane crossflow microfiltration of oil emulsion, Desalination 127 (2000) 189–198.